

A Conical Intersection Mechanism for the Photochemistry of Butadiene. A MC-SCF Study

Massimo Olivucci,^{*†} Ioannis N. Ragazos,[‡] Fernando Bernardi,[†] and Michael A. Robb^{*‡}

Contribution from the Dipartimento di Chimica "G. Ciamician" dell'Università di Bologna, Via Selmi 2, 40126 Bologna, Italy, and the Department of Chemistry, King's College, London, Strand, London WC2R 2LS, U.K.

Received August 5, 1992

Abstract: The excited state (2^1A_g) reaction paths involved in the photochemical transformations of butadiene have been studied via ab initio MC-SCF methods. It is demonstrated that the reaction funnel assumes the form of a conical intersection region where the ground (1^1A_g) and first excited (2^1A_g) potential energy surfaces are degenerate. This mechanism is consistent with experimental results for the photochemical isomerization and is also consistent with the observed absence of fluorescence from the 2^1A_g state. Thus the currently accepted mechanisms for butadiene photochemistry which involve radiationless decay at avoided crossing minima need to be replaced with a model that involves fully efficient return to the ground state via a conical intersection. In addition to the minima on the excited state surface, the lowest energy points on the conical intersection region have been fully optimized. The conical intersection points have been characterized by computing the gradient difference and non-adiabatic coupling vectors. Reaction paths from the excited state minima to these conical intersections have been computed. The lowest energy path from the *s-trans* minimum on the 2^1A_g potential energy surface involves the rotation of the central C–C bond coupled with asynchronous disrotatory motion of the terminal methylenes and leads to an *s-transoid* conical intersection region without passing over a barrier. The reaction path from the *s-cis* minimum leads to an *s-cisoid* conical intersection that lies some 4 kcal mol⁻¹ above this minima. The nature of the possible reaction paths on the excited state is consistent with the fact that the major products of the photochemical reactions of butadiene are *s-cis/s-trans* isomerization and double bond *cis/trans* isomerization. These findings are also consistent with the directions of the gradient difference and non-adiabatic coupling vectors computed at a point where the system enters the conical intersection. In particular, the directions of these two vectors near the *s-cisoid* conical intersection are consistent with the production of cyclobutane as minor product.

1. Introduction

In ground-state reactivity the mechanistic explanation for the simultaneous production of different products starting from a single reactant is usually formulated on the basis of the existence of competing reaction pathways on the ground-state potential energy surface. Each pathway starts at the minimum of the potential energy corresponding to the reactant molecule and leads to a different product via passage through a pathway-specific transition structure. In the past, the same argument has been used to rationalize excited state reactivity problems. The essential difference is that a photochemical reaction is, in general, non-adiabatic and the excited state pathway must lead to a Born–Oppenheimer violation region where radiationless relaxation to the ground state (for instance via internal conversion¹) occurs near the corresponding product. After this relaxation the system follows a ground-state path ending at the photoproduct structure.

In the past, this kind of mechanism has been used to rationalize the photochemical behavior of butadienes.^{1–22} In butadiene

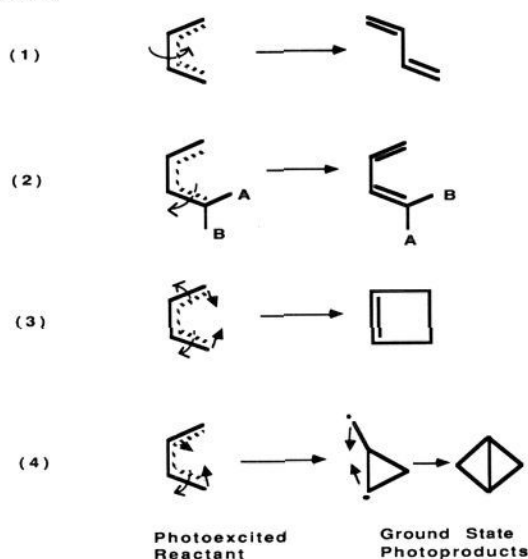
photochemistry, the assumed or proposed reaction paths associated with the observed photoproducts are, in general, very different since their corresponding reaction coordinates are dominated by different geometrical parameters. For example, while the assumed reaction coordinate for the *s-cis/s-trans* isomerization (eq 1 in Scheme I) involves rotation about the central C–C bond, the proposed reaction coordinate for the *cis/trans* double bond isomerization (eq 2 in Scheme I)^{4,19,20} involves rotation of a single terminal methylene while the carbon framework of the structure remains almost unchanged. In contrast, the cyclization of *s-cis*-butadiene^{3,4,7,18} involves mainly bending of the carbon framework plus rotation of both of the two terminal methylenes (eq 3 in Scheme I). Finally the proposed reaction coordinate for bicyclobutane formation (eq 4 in Scheme I) is dominated by an initial *cis/trans* double bond isomerization followed by bending and twisting of the σ framework and leading to a ground-state cyclopropane intermediate.^{7–11}

The central mechanistic question associated with a non-adiabatic photochemical reaction relates to the location of the reaction funnel^{18,23–25} which separates the part of a reaction path that lies on the excited state and the part that lies on the ground state. At this point the system must undergo radiationless decay

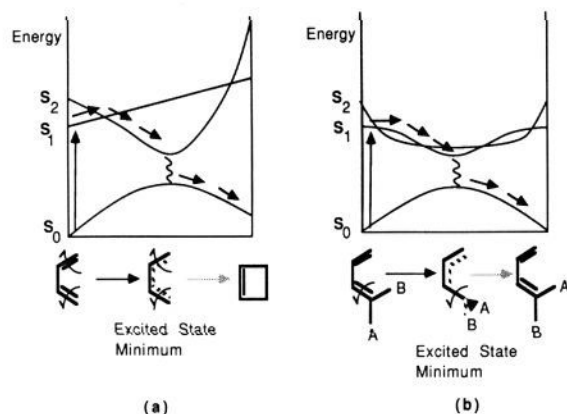
[†] Dipartimento Chimico "G. Ciamician" dell'Università di Bologna.
[‡] Chemistry Department, King's College London.
 (1) Gilbert, A.; Baggott, J. *Essentials of Molecular Photochemistry*; Blackwell Scientific Publications: Oxford, 1991.
 (2) Coxson, J. M.; Halton, B. *Organic Photochemistry*; Cambridge University Press: London, 1974; pp 47.
 (3) Fonken, G. J. Photochemistry of olefins. In *Organic Photochemistry*; Chapman, O. L., Ed.; Marcel Dekker, Inc.: New York, 1967.
 (4) Squillacote, M.; Semple, T. C. *J. Am. Chem. Soc.* **1990**, *112*, 5546.
 (5) Squillacote, M. E.; Semple, T. C.; Mui, P. W. *J. Am. Chem. Soc.* **1985**, *107*, 6842.
 (6) Squillacote, M. E.; Sheridan, R. S.; Chapman, O. L.; Anet, F. A. L. *J. Am. Chem. Soc.* **1979**, *101*, 3657.
 (7) Srinivasan, R. *J. Am. Chem. Soc.* **1968**, *90*, 4498.
 (8) Srinivasan, R. *J. Am. Chem. Soc.* **1961**, *83*, 2807.
 (9) Srinivasan, R. *J. Am. Chem. Soc.* **1962**, *84*, 3982.
 (10) Dauben, W. G.; Ritscher, J. S. *J. Am. Chem. Soc.* **1970**, *92*, 2925.
 (11) Gale, D. M. *J. Org. Chem.* **1970**, *35*, 970.

(12) Aue, D. H.; Reynolds, R. N. *J. Am. Chem. Soc.* **1973**, *95*, 2027.
 (13) Kelso, P. A.; Yeshurum, A.; Shih, C. N.; Gajewski, J. J. *J. Am. Chem. Soc.* **1975**, *97*, 1513.
 (14) Bigwood, M.; Boue, S. *J. Chem. Soc., Chem. Commun.* **1974**, *92*, 529.
 (15) Boue, S.; Srinivasan, R. *J. Am. Chem. Soc.* **1970**, *92*, 3226.
 (16) Trulson, M. O.; Mathies, R. A. *J. Phys. Chem.* **1990**, *94*, 5741.
 (17) Woodward, R. B.; Hoffmann, R. *Angew. Chem., Int. Ed. Engl.* **1969**, *8*, 781.
 (18) Van der Lugt, W. T. A. M.; Oosterhoff, L. J. *J. Am. Chem. Soc.* **1969**, *91*, 6042.
 (19) Aoyagi, M.; Osamura, Y. *J. Am. Chem. Soc.* **1989**, *111*, 470.
 (20) Aoyagi, M.; Osamura, Y. *J. Chem. Phys.* **1985**, *83*, 1140.
 (21) Zerbetto, F.; Zgierski, M. Z. *J. Chem. Phys.* **1990**, *93*, 1235.
 (22) Morihashi, K.; Kikuchi, O. *Theor. Chim. Acta* **1985**, *67*, 293.

Scheme I



Scheme II

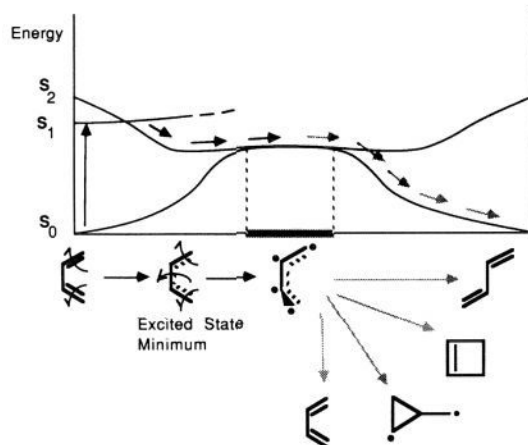


from the excited state to the ground state. The currently accepted model¹⁸ assumes that this decay occurs from the *avoided crossing minimum* that occurs on the excited state. The efficiency of this decay is determined mainly by the *gap* between ground and excited state potential energy surfaces at this point.

In butadiene photochemistry, the accepted mechanism for the cyclization of *s-cis* butadiene (Scheme IIa) is that proposed by Oosterhoff et al.¹⁸ This mechanism involves an excited state branch corresponding to *in-plane* bending of the carbon framework plus synchronous¹⁸ (or asynchronous⁴) rotation of both of the two terminal methylenes leading to an (avoided crossing) minimum and then, on the ground-state branch, following internal conversion, one has ring closure or motion back to reactants. Further, it is assumed that the carbon framework of the system remains planar along the reaction pathway and thus the reaction path is different from the reaction path leading to *s-cis/s-trans* isomerization (see eq 1 in Scheme I). The proposed reaction coordinate for the *cis/trans* double bond isomerization^{4,19,20} (Scheme IIb) involves an initial rotation of a single terminal methylene by 90.0° on the excited state branch (while the rest of the structure remains almost unchanged) leading again to an excited state minimum. The remainder of the rotation occurs on the ground state branch following internal conversion from the excited state minimum. For both reactions a and b in Scheme II as well as for the *s-cis/s-trans* isomerization the reaction *funnels* are assumed to be different excited state minima located along different paths connecting reactants and products.

The lowest energy singlet electronic states of 1,3-dienes are the one-photon allowed 1^1B_u state (single excitation from HOMO

Scheme III



to LUMO of the π system, S_1 in Scheme IIa) and the 2^1A_g state (double excitation from HOMO to LUMO, S_2 in Scheme IIa). Recent experimental work¹⁶ has shown that internal conversion from the 1^1B_u to the 2^1A_g state competes effectively with vibrational relaxation on the 1^1B_u surface so that the photochemical reactions of 1,3-dienes occur from the 2^1A_g state. Thus we shall focus our attention on the 2^1A_g state.

In the present paper, we shall present a detailed view of the excited state potential energy surface for butadiene and demonstrate the existence of an accessible conical intersection region.²⁶⁻⁴⁴ As a consequence of these detailed results, we shall show that the currently accepted Oosterhoff model¹⁸ discussed above needs to be replaced with a new and more general mechanistic scheme which we now briefly introduce. The most important aspect of this new model (that was in fact suggested in early model computations on H_4 ²³ and is documented in detail for the first time in the present paper) is the proposal that the reaction *funnel* assumes the form of a conical intersection point²⁶⁻³⁵ where the ground (1^1A_g) and first excited (2^1A_g) potential energy surfaces (S_0 and S_2 in Schemes II and III) are degenerate (see the central part of Scheme III). The central feature of the mechanistic scheme to be documented in this paper is that along

(23) Gerhartz, W.; Poshusta, R. D.; Michl, J. *J. Am. Chem. Soc.* **1977**, *99*, 4263.

(24) Michl, J.; Bonacic-Koutecky, V. *Electronic Aspects of Organic Photochemistry*; Wiley: New York, 1990.

(25) Bonacic-Koutecky, V.; Koutecky, J.; Michl, J. *Angew. Chem., Int. Ed. Engl.* **1987**, *26*, 170.

(26) Von Neumann, J.; Wigner, E. *Physik. Z.* **1929**, *30*, 467.

(27) Teller, E. *J. Phys. Chem.* **1937**, *41*, 109.

(28) Herzberg, G.; Longuet-Higgins, H. C. *Trans. Faraday Soc.* **1963**, *35*, 77.

(29) Herzberg, G. *The Electronic Spectra of Polyatomic Molecules*; Van Nostrand: Princeton, 1966; pp 442.

(30) Mead, C. A.; Truhlar, D. G. *J. Chem. Phys.* **1979**, *70*, 2284.

(31) Mead, C. A. *Chem. Phys.* **1980**, *49*, 23.

(32) Keating, S. P.; Mead, C. A. *J. Chem. Phys.* **1985**, *82*, 5102.

(33) Keating, S. P.; Mead, C. A. *J. Chem. Phys.* **1987**, *86*, 2152.

(34) Davidson, R. E.; Borden, W. T.; Smith, J. *J. Am. Chem. Soc.* **1978**, *100*, 3299.

(35) Mead, C. A. The Born-Oppenheimer approximation in molecular quantum mechanics, In *Mathematical frontiers in computational chemical physics*; Truhlar, D. G., Ed.; Springer: New York, 1987; Chapter 1, pp 1-17.

(36) Tully, J. C.; Preston, R. K. *J. Chem. Phys.* **1971**, *55*, 562.

(37) Dehareng, D.; Chapuisat, X.; Lorquet, J. C.; Galloy, C.; Raseev, G. *J. Chem. Phys.* **1983**, *78*, 1246.

(38) Blais, N. C.; Truhlar, D. G.; Mead, C. A. *J. Chem. Phys.* **1988**, *89*, 6204.

(39) Manthe, U.; Koppel, H. *J. Chem. Phys.* **1990**, *93*, 1658.

(40) Salem, L. *Electrons in Chemical Reactions: First Principles*; Wiley: New York, 1982.

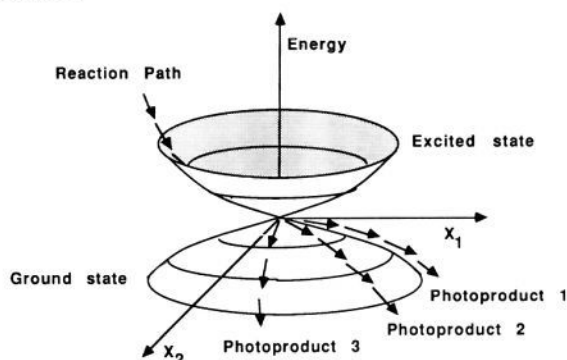
(41) Bernardi, F.; De, S.; Olivucci, M.; Robb, M. A. *J. Am. Chem. Soc.* **1990**, *112*, 1737.

(42) Bernardi, F.; Olivucci, M.; Robb, M. A. *Acc. Chem. Res.* **1990**, *23*, 405.

(43) Bernardi, F.; Olivucci, M.; Robb, M. A. *J. Am. Chem. Soc.*, in press.

(44) Bernardi, F.; Olivucci, M.; Ragazos, I. N.; Robb, M. A. *J. Am. Chem. Soc.* **1992**, *114*, 2752.

Scheme IV



the *s-cis/s-trans* excited state isomerization pathway (involving simultaneous rotation about the central C–C bond of the butadiene carbon framework and asynchronous disrotatory rotation of the two terminal methylenes) one does not find any conventional intermediate or transition structure. Rather, one finds a conical intersection region where the excited state and the ground state potential energy surface are degenerate (see the central part of Scheme III). Furthermore, as we will report in section 3, the absolute minimum energy point of the excited state potential energy surface is not the expected *avoided crossing minimum* but instead it coincides with a *conical intersection point* where ground and excited states are degenerate. Consequently, while the excited state branch of the reaction coordinate (from either *s-cis* or *s-trans* excited state butadiene) corresponds to *s-cis/s-trans* isomerization of the excited state reactant, this isomerization process is not completed because the reacting system is funneled to the ground state through the conical intersection about one-third of the way along the pathway.

The very existence of a conical intersection is of central importance for two reasons. Firstly, at this point a fully efficient radiationless decay from the excited state to the ground state becomes possible (i.e., $E_1 - E_2 = 0$). (It has been demonstrated for realistic systems that the decay occurs rapidly within less than a vibrational period [see for example ref 39].) In contrast, in the Oosterhoff model, the decay occurs from an avoided crossing minimum so that the decay rate is controlled by the energy gap and there is the possibility of competition with other slower events such as fluorescence. Secondly, the existence of this type of conical intersection region provides access to a limited number of low-energy ground-state pathways that can lead to different photoproducts. These pathways originate from the same conical intersection point via a “bifurcation” of the excited state reaction path as schematically illustrated on the right-hand side of Scheme III. This situation is a consequence of the nature and shape of the touching region of the ground/excited state surfaces (the shape of the region surrounding a conical intersection point resembles that of a double cone) illustrated in Scheme IV. The initial ground-state-reactive trajectories are located in the x_1x_2 plane (in Scheme IV) in the immediate region of the apex of the cone. Afterwards, as one moves away from it, the potential energy gets lowered in a number of particular directions to generate reaction valleys (i.e. a reaction pathway) leading to one of the possible photoproducts. (As we shall discuss in detail in the next section, these two directions x_1x_2 are precisely defined as the gradient difference vector and non-adiabatic coupling vector between the ground (1^1A_g) and excited (2^1A_g) states.) In summary, the knowledge of both the molecular structure associated with the conical intersection point and the type of molecular motion in the x_1x_2 plane centered on it provides the information for rationalizing the nature of the decay process and the nature of the initial motion on the ground state. In this work we have optimized the molecular structure of lowest energy conical intersections for butadiene and characterized them by computing, from *ab initio* MC-SCF wave functions, the two directions x_1 and

x_2 , and thus we can document the effects discussed above in a rigorous way.

Thus our purpose in this paper is to document the photochemical mechanism of butadiene as an example of the photochemistry of butadienes in general and to show that the Oosterhoff¹⁸ model which involves decay from an avoided crossing minimum must be replaced by a model where the *funnel* is a conical intersection. We shall show that the geometries of the conical intersections and a knowledge of the directions of the gradient difference vector and the non-adiabatic coupling vector are of central importance in understanding the photochemistry of these compounds. In section 2 we briefly summarize the procedure used to study the conical intersection region. In the following section (section 3) we document the *global* structure of the ground and excited state potential energy surfaces using a new semiquantitative simulation technique that combines a VB model with molecular mechanics methods (MM-VB^{45,46}). Finally, in section 4, we shall discuss the detailed nature of the mechanism on the basis of *ab initio* MC-SCF computations on ground and excited states.

2. Optimization and Characterization of Conical Intersections

While the location of minima and transition states is readily accomplished using standard methods, the location of the “funnel” from the excited state surface to the ground state surface that corresponds to a conical intersection requires nonstandard methods. Thus it is appropriate to give some discussion at this point.

A detailed mathematical discussion of conical intersections can be found in refs 30–35. A discussion from a more chemical point of view can be found in the book of Michl²⁴ and in refs 25–34. In two previous papers^{41,42} we have discussed a VB model for the conical intersection of two potential energy surfaces for a system with 4 active orbitals (i.e. those involved in bond breaking/making) and 4 electrons in some detail. Here we briefly outline the numerical procedure used to optimize the conical intersection geometries and to characterize such points in terms of two vectors x_1 and x_2 .

A conical intersection is defined by the following statement:⁴⁰ *Two states even with the same symmetry will intersect along a $(n - 2)$ -dimensional hyperline as the energy is plotted against the n internal nuclear coordinates.* We are interested in the lowest energy stationary points on this hyperline which correspond to well-defined optimized geometries of the system. In order to properly locate these low-energy stationary points where two potential energy surfaces have the same energy, one must carry out constrained geometry optimizations on the excited state potential energy surface where the geometry is optimized in directions orthogonal to the two directions x_1 and x_2 (illustrated in Scheme IV). Thus, the two directions x_1 and x_2 “characterize” a conical intersection point in the sense that the energy degeneracy is removed for any finite step in the plane defined by x_1 and x_2 . As shown in Scheme IV, the conical intersection region is a point on this plane and thus any distortion from the structure corresponding to this point will lift the degeneracy. In other words, in order to locate the most “stable” conical intersection structures, we simply search for a local minimum on a $(n - 2)$ -dimensional cross section of the n -dimensional potential energy surface which corresponds to a $(n - 2)$ -dimensional hyperline orthogonal to the plane of x_1 and x_2 . It is important to appreciate that the gradient on the excited state potential energy surface will not be zero at a conical intersection point, since it “looks like” the vertex of an inverted cone. Rather, it is the projection of the gradient of the excited state potential energy surface onto the orthogonal complement of x_1 and x_2 (i.e. $(n - 2)$ -dimensional hyperline) that goes to zero when the geometry of the conical intersection is optimized. This situation is distinguished from an

(45) Bernardi, F.; Olivucci, M.; McDouall, J. J. W.; Robb, M. A. *J. Chem. Phys.* **1988**, *89*, 6365.

(46) Bernardi, F.; Olivucci, M.; Robb, M. A. *J. Am. Chem. Soc.* **1992**, *114*, 1606.

“avoided crossing minimum” of two surfaces where the gradient on the excited state potential energy surface would go to zero.

The actual algorithm used to optimize the conical intersection is similar to that suggested by Morokuma et al.,⁴⁷ and we have presented the details of our approach elsewhere.⁴⁸ Here we shall be content to define \mathbf{x}_1 and \mathbf{x}_2 and discuss their physical significance. The vector \mathbf{x}_1 corresponds to the gradient difference

$$\mathbf{x}_1 = \frac{\partial(E_1 - E_2)}{\partial \mathbf{s}} \quad (1)$$

and \mathbf{x}_2 corresponds to the non-adiabatic coupling

$$\mathbf{x}_2 = \left\langle \Psi_1 \left| \frac{\partial \Psi_2}{\partial \mathbf{s}} \right. \right\rangle \quad (2)$$

where $\delta \mathbf{s}$ is an infinitesimal nuclear displacement vector. They are easily computed using state averaged orbitals in the manner suggested by Yarkony.⁴⁹ At a point near the conical intersection, \mathbf{x}_1 will point to the apex of the cone. In particular, if this point lies on the bottom of an excited state valley (reaction path) entering the conical intersection region, then \mathbf{x}_1 will be parallel to the reaction path defined by that valley. The vector \mathbf{x}_2 would be, in general, nearly orthogonal to \mathbf{x}_1 and therefore \mathbf{x}_2 will be nearly orthogonal to the same excited state reaction path.

As suggested in the previous section, the two vectors \mathbf{x}_1 and \mathbf{x}_2 have a dynamic significance which can be discussed qualitatively in the framework of the trajectory surface hopping (TSH) treatment^{36–38} of the excited state/ground state decay process. The system, after absorption of a photon, will leave the Franck–Condon region or excited state minima along a bundle of classical trajectories which will be mainly located at the bottom of valleys (i.e. pathways) existing on the excited state potential energy surface and leading toward the conical intersection region. In fact, in this part of the excited state surface the energy separation between ground and excited state is still too large to allow surface hop and the motion of the system will be controlled by the structure of the surface in a classical fashion. At the end of this pathway the system will enter the Born–Oppenheimer violation region centered on the conical intersection point where the energy gap is small and consequently the probability of a surface hop is large. The system enters this region with a momentum oriented in the direction of the pathway which is approximately parallel to vector \mathbf{x}_1 (\mathbf{x}_1 points at the apex of the cone) and then undergoes surface hop to the ground state. The direction of the motion will not be, in general, conserved in this process since *the effective direction for the surface hop* is taken to be parallel to the direction of the non-adiabatic coupling matrix element \mathbf{x}_2 ^{36–38} as defined in eq 2 which is nearly orthogonal to \mathbf{x}_1 . So when the surface hop occurs, in order to conserve total energy, one must adjust one component of the momentum in the “direction” of the non-adiabatic coupling vector. Thus, the initial direction of motion (i.e. the initial trajectory) after the excited state/ground state decay will be determined by a combination of the original momentum existing on the excited state pathway (i.e. directed toward the apex of the cone and parallel to \mathbf{x}_1) at the moment when the system enters the conical intersection region with this second component parallel to \mathbf{x}_2 . While one could, in principle, run dynamics calculations for determining the most probable direction for the surface hop (i.e. the actual combination of the momenta parallel to \mathbf{x}_1 and \mathbf{x}_2), the initial directions of motion will all lie on the plane $\mathbf{x}_1\mathbf{x}_2$ as shown in Scheme IV. As we will discuss in the results section of this paper, qualitative information on the nature of the possible initial ground-state trajectories can be inferred from the characteristics of the plane $\mathbf{x}_1\mathbf{x}_2$ alone.

From a practical point of view, when we optimize the geometry of a conical intersection, we end up at an arbitrary point in the immediate vicinity of the apex of the cone and not necessarily in

a point along the excited state path leading to the conical intersection point. Thus, in general, it is incorrect to attribute any dynamic significance to \mathbf{x}_1 and \mathbf{x}_2 independently if they are computed in such an arbitrary point; only the plane spanned by these vectors has any meaning. In fact, as pointed out above, this plane contains all possible directions of the initial motion of the system for the ground-state relaxation process.

Now we discuss the mechanistic significance of a conical intersection. In Scheme II we have illustrated the way in which the Oosterhoff model associates a different reaction funnel (via an avoided crossing minimum) with *each* possible reaction path. In the model proposed in this paper we show that the conical intersection region provides a *single* topological feature of the excited and ground state surfaces which can lead to *several* possible products. In order to appreciate the special role of a conical intersection as a transition point between the excited and ground state in a photochemical reaction, it is useful to draw an analogy with a transition state in a thermal reaction. In a thermal reaction, one characterizes the transition state with a single vector that corresponds to the reaction path through the saddle point. The transition structure is a minimum in all coordinates except the one that corresponds to the reaction path. In Scheme IV we have shown the double cone topology that occurs in the directions \mathbf{x}_1 and \mathbf{x}_2 at points that lie in the conical intersection region (energy of ground and excited state are equal). The system must assume a geometry near that of the conical intersection or the decay probability is vanishingly small. Further one can make the following statement: *The optimized geometry of a low-energy point on a conical intersection is characterized by two vectors rather than one and the initial trajectory in the immediate vicinity of the apex of the cone (for infinitely slow nuclear motion on the ground-state surface) must lie in the plane defined by these two vectors.* The energy of the excited state is a minimum in all coordinates except \mathbf{x}_1 and \mathbf{x}_2 . As a consequence, while a transition state for a thermal reaction provides a single direction for the reaction path, a conical intersection provides *two possible linearly independent* reaction path directions in the immediate vicinity of the apex of the cone that must lie in the $\mathbf{x}_1\mathbf{x}_2$ plane.

While the family of initial ground-state trajectories will lie in the plane $\mathbf{x}_1\mathbf{x}_2$, the actual ground-state reaction path that the system would follow also must be determined by the accessibility of ground-state valleys which may develop, as one moves away from the apex of the cone, which control the direction of the motion during the ground-state relaxation and lead to the photoproduct minima. However, the detailed course of the reaction must be determined by dynamical considerations and one should run quantitative dynamical calculations^{36–38} in order to get an estimate of the relative quantum yields for the various photoproducts.

3. Global Structure of the Excited State Reaction Surface

While we can optimize the geometries of the conical intersection points and other critical points using rigorous ab initio MC-SCF calculations, the global structure of the low-energy part of the 2^1Ag excited state potential energy surface for the butadiene molecule can only be visualized by plotting the energy on a grid. Computing grids of energy values with ab initio methods is rather expensive, thus we use the newly developed⁴⁶ MM-VB (molecular mechanics with valence bond) method for this purpose. This technique provides a very low-cost but effective tool for investigating the structure of ground and excited state potential energy surfaces for organic reactions. As we have demonstrated in different examples,⁴⁶ MM-VB correctly reproduces the shape (topology) of ab initio MC-SCF potential energy surfaces.

Our objective in this section is to illustrate the various reaction paths and minima for butadiene isomerization within a three-dimensional cross section of the excited state potential energy surface (defined by the box in Figure 1) spanning the three possible rotations ($\alpha_1, \alpha_2, \beta$) about the three C–C bonds in the butadiene

(47) Morokuma, K.; Koga, N. *Chem. Phys. Lett.* **1985**, *119*, 371.

(48) Ragazos, I. N.; Robb, M. A.; Bernardi, F.; Olivucci, M. *Chem. Phys. Lett.* **1992**, *197*, 217.

(49) Yarkony, D. R. *J. Chem. Phys.* **1990**, *92*, 2457.

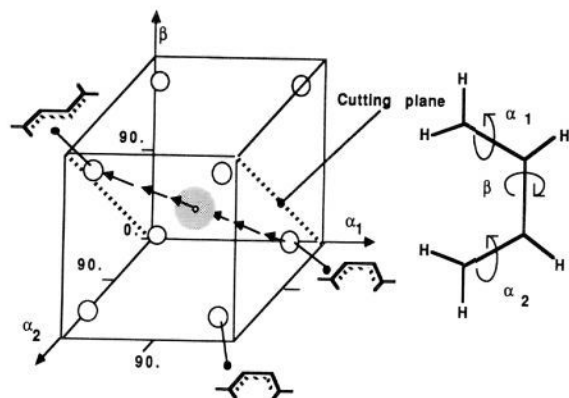


Figure 1. Global structure of a three-dimensional cross section of the excited state potential energy surface for butadiene. The coordinates α_1 , α_2 , and β correspond to rotations about the three C–C σ bonds of the butadiene framework and span a range from 0 to 180°. The circles represent the location of excited state stable structures found inside the cross section while the dotted central volume represents the conical intersection region centered on the (90,90,90) point. The diagonals of the cutting plane shown inside the box correspond to conrotatory and disrotatory (denoted by arrows) hypothetical pathways going from the *s*-cis to the *s*-trans minimum.

moiety. The variable β describes the *s*-cis/*s*-trans isomerization process, and the coordinates α_1 and α_2 describe the *cis*/*trans* isomerization of the two terminal double bonds which can change in both a synchronous and an asynchronous fashion when β is approaching a value of 90°. The grid of values has been generated by changing the values of the three geometrical parameters α_1 , α_2 , and β through a range of 180°. We have used a $20 \times 20 \times 20$ grid of potential energy values, choosing as the origin of the grid the structure corresponding to a planar excited state *s*-cis-butadiene (whose geometrical parameters had been previously optimized under the planar constraint). This gives a global view of the surface which will be presented in a more refined but less detailed fashion in the ab initio MC-SCF study later.

We shall be content with a general summary of these results and we will only discuss the energy profile in the "cutting plane" indicated in Figure 1 in detail. The center of the box (90,90,90) in Figure 1 which we have shaded corresponds to a point with all the π bonds twisted by 90°. This is the conical intersection region which we will document in detail subsequently with ab initio results. The position of the *s*-cis and *s*-trans minima corresponding to the excited state butadiene are indicated by circles near the bottom face and the top face of the box, respectively. The visualization of the two stereochemically different pathways for the excited state *s*-cis/*s*-trans isomerization is the central objective of these computations and can be accomplished by plotting potential energy surfaces in the special cutting plane defined by dashed lines in Figure 1. This cutting plane contains both the disrotatory and conrotatory approaches to the conical intersection region. The disrotatory pathway corresponds to the one represented in the central part of Scheme III, and in Figure 1 it is marked by a stream of arrows. The conrotatory pathway is located along the other diagonal of the cutting plane. Two potential energy surfaces obtained in this cutting plane are shown as elevated contour plots in Figure 2.

Figure 2a illustrates the behavior of the energy difference between the ground (1^1A_g) and excited (2^1A_g) states along this cross section. The central deep minimum of the surface corresponds to a value of $E_1 - E_2 = 0$ which illustrates the presence of a conical intersection area centered on the (90,90,90) point. The difference in energy increases going from the center toward the edges of the surface where the excited and ground state potential energy surfaces are well separated and where the four (two *s*-cis and two *s*-trans) excited state minima are located. Figure 2b illustrates the behavior of the total energy E_2 of the excited state. One can see that despite the general flatness of this

potential energy surface, there are four minima located near the four corners of the surface and corresponding to two *s*-cis and two *s*-trans excited state butadienes. Further, there exists a disrotatory pathway for infinitely slow nuclear motion that corresponds to the most favorable pathway for converting an *s*-cis-butadiene to an *s*-trans-butadiene which passes via the central (90,90,90) point where the conical intersection region is located. Thus the most important observation that can be made from this potential energy surface is that the conrotatory and disrotatory pathways are not equivalent pathways for the *s*-cis/*s*-trans isomerization and the disrotatory pathway to the conical intersection region involves a lower barrier route. Furthermore, this route does not correspond to a synchronous CH₂ disrotatory rotation of the two methylenes (the pathway does not run along the diagonal of the cross section) but it seems to involve a faster rotation of one of the two methylenes.

4. Ab Initio Results for Excited State Minima and Optimized Conical Intersections

We shall now confirm our predictions using rigorous ab initio MCSCF/4-31G results for the first excited state of butadiene. Our investigation is limited to the low-energy part of the corresponding potential energy surface where the system, after absorption of a photon, would relax from the Franck–Condon region. It is our intention to fully document the detailed features of the mechanism proposed in section 1 and illustrated globally in section 3.

Since we are interested in the delicate interplay of the ground (1^1A_g) and first excited (2^1A_g) potential energy surfaces of butadiene, SCF (restricted or unrestricted) cannot give a correct zeroth-order description of the problem. Accordingly we have used a modified version of the implementation of the MC-SCF method^{50–52} distributed in GAUSSIAN.^{53,54} In MC-SCF the orbitals for an excited state can be optimized using higher roots of the CI eigenvalue problem. In this problem the choice of the active orbitals is completely unambiguous: the 4 $p\pi$ orbitals that correlate with the π system in planar butadiene. The 4-31G basis has been used for all computations.

A fairly complete ab initio MC-SCF/STO-3G study of the excited states of butadiene has been published already by Aoyagi and Osamura.^{19,20} These authors have reported optimized structures of four excited state minima lying on the first singlet excited state which has been found to correspond to a doubly excited ($2^1A_g/2^1A$) state. The first two minima correspond to two different conformations (C_2 and S_2 symmetry) of *s*-trans butadiene while the remaining two are conformations of *s*-cis butadiene (C_2 and C_s symmetry). However, no study with optimized transition structures has been reported for the *s*-cis/*s*-trans isomerization or the double bond *cis*/*trans* isomerization on the excited state surface. In order to get a more accurate and complete picture of the excited state potential energy surface we have investigated a large region which includes not only the *s*-cis and *s*-trans conformer basins but also the *s*-cis/*s*-trans transition regions where the torsional angle about the central C–C bond (β in Figure 1) has values around 90°. In particular, we have investigated the existence of both reaction pathways and transition structures connecting the *s*-cis to the *s*-trans basins. The only excited state (2^1A_g) butadiene geometries which have been found

(50) Eade, R. H. A.; Robb, M. A. *Chem. Phys. Lett.* **1981**, *83*, 362.

(51) Schlegel, H. B.; Robb, M. A. *Chem. Phys. Lett.* **1982**, *93*, 43.

(52) Frisch, M.; Ragazos, I. N.; Robb, M. A.; Schlegel, H. B. *Chem. Phys. Lett.* **1992**, *189*, 524.

(53) *Gaussian 91* (Revision C), Frisch, M. J.; Head-Gordon, M.; Trucks, G. W.; Foresman, J. B.; Schlegel, H. B.; Raghavachari, K.; Robb, M.; Wong, M. W.; Replegle, E. S.; Binkley, J. S.; Gonzalez, C.; Defrees, D. J.; Fox, D. J.; Baker, J.; Martin, R. L.; Stewart, J. J. P.; and Pople, J. A. Gaussian, Inc., Pittsburgh, PA, 1991.

(54) *Gaussian 90*, Frisch, M. J.; Head-Gordon, M.; Trucks, G. W.; Foresman, J. B.; Schlegel, H. B.; Raghavachari, K.; Robb, M.; Binkley, J. S.; Gonzalez, C.; Defrees, D. J.; Fox, D. J.; Whiteside, R. A.; Seeger, R. A.; Melius, C. F.; Baker, J.; Martin, R. L.; Kahn, L. R.; Stewart, J. J. P.; Topiol, S.; and Pople, J. A. Gaussian, Inc., Pittsburgh, PA, 1990.

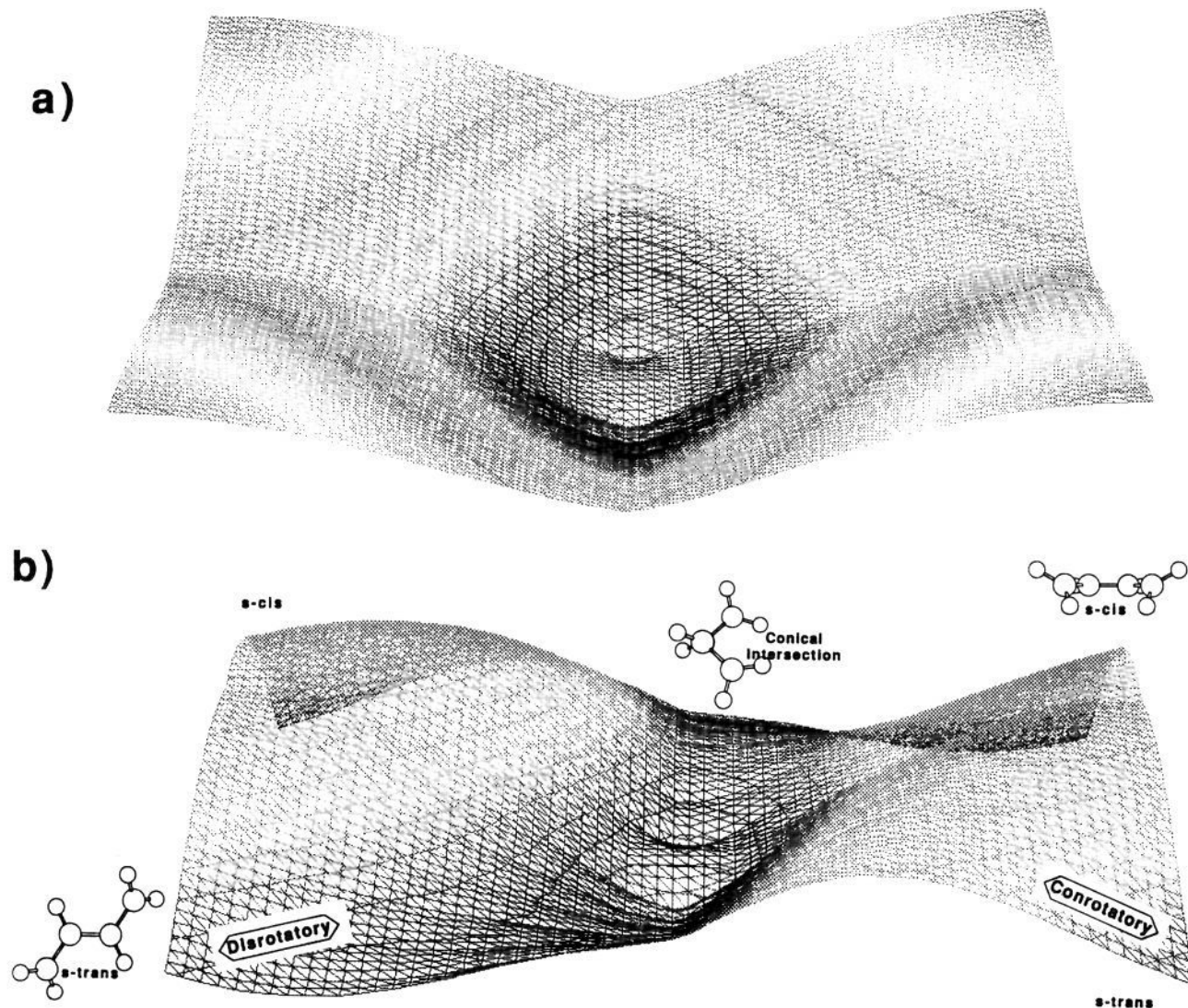


Figure 2. Behavior of the quantities $E_2 - E_1$ (a) and E_2 (b) along the cutting plane defined in Figure 1. The energy values have been obtained via MM-VB simulation. Note that since the C-C-C-C torsional angle at the conical intersection is 84° there are two equivalent conical intersections located at the middle of each surface.

Table I. Energies of Geometries on Ground and Excited State Potential Energy Surfaces of Butadiene

structure		E_2	$E_2(\text{SA})$	$E_2(\text{SA}) - E_1(\text{SA})$
C_2 s-cis min	a	-154.5634	-154.5623	0.121
C_s s-cis min	b	-154.5654	-154.5640	0.111
C_2 s-trans min	c	-154.5641	-154.5627	0.115
S_2 s-trans min	d	-154.5638	-154.5627	0.111
C_2/C_s s-cis TS	e	-154.5622		
C_2/S_2 s-trans TS	f	-154.5619		
central CI	g		-154.5540	
s-cisoid CI	h		-154.5580	0.0005
s-transoid CI	i		-154.5689	0.0001

previously using the same method and level of theory used in this work correspond to different conformations of the *s-trans*-butadiene,²¹ namely, one C_2 and one S_2 *s-trans* conformations, while no *s-cis* conformer structures have been characterized.

The energetics (see Table I) and geometries of the equilibrium structures found at the MC-SCF/4-31G level of theory are qualitatively in agreement with the results reported by Aoyagi and Osamura.^{19,20} The two stable *s-cis* conformations correspond to C_2 and C_s symmetry (Figure 3a/b, respectively), and, like the two *s-trans* conformations (C_2 and S_2 symmetry) (Figure 3c/d, respectively), have almost equal energies. In Figure 3e/f we

have also reported two conformational transition structures, i.e. C_2/C_s and C_2/S_2 , connecting the two *s-cis* and the two *s-trans* conformers respectively and placed at less than 1 kcal/mol above the stationary points. This barrier height suggests that each pair of conformers can easily interconvert even at very low temperature.

Because the stationary points shown in Figure 3a-f are located on the bottom of the two shallow *s-cis* and *s-trans* basins, one needs to search for possible transition structures connecting these two basins. One could relate, via a least motion path, the C_2 *s-cis* conformer to the C_2 *s-trans* conformer and the C_s *s-cis* conformer to the S_2 *s-trans* conformer via rigid rotation about the central C-C bond of butadiene. However, such idealized adiabatic *s-cis*/*s-trans* reaction pathways do not exist on the excited state surface. Rather, in agreement with the global results obtained in the preceding section, in the *s-cis*/*s-trans* transition region there is no real transition structure for the *s-cis*/*s-trans* isomerization process, rather one finds only points where the first excited state and the ground state are degenerate. Thus one has a large contiguous region of "touching" between the ground and excited state potential energy surfaces along the *s-cis*/*s-trans* isomerization path. We have fully optimized three quite different critical points on this conical intersection region, denoted as *s-transoid*, *s-cisoid*, and "central", and characterized these structures using the gradient difference and the non-adiabatic coupling vector at

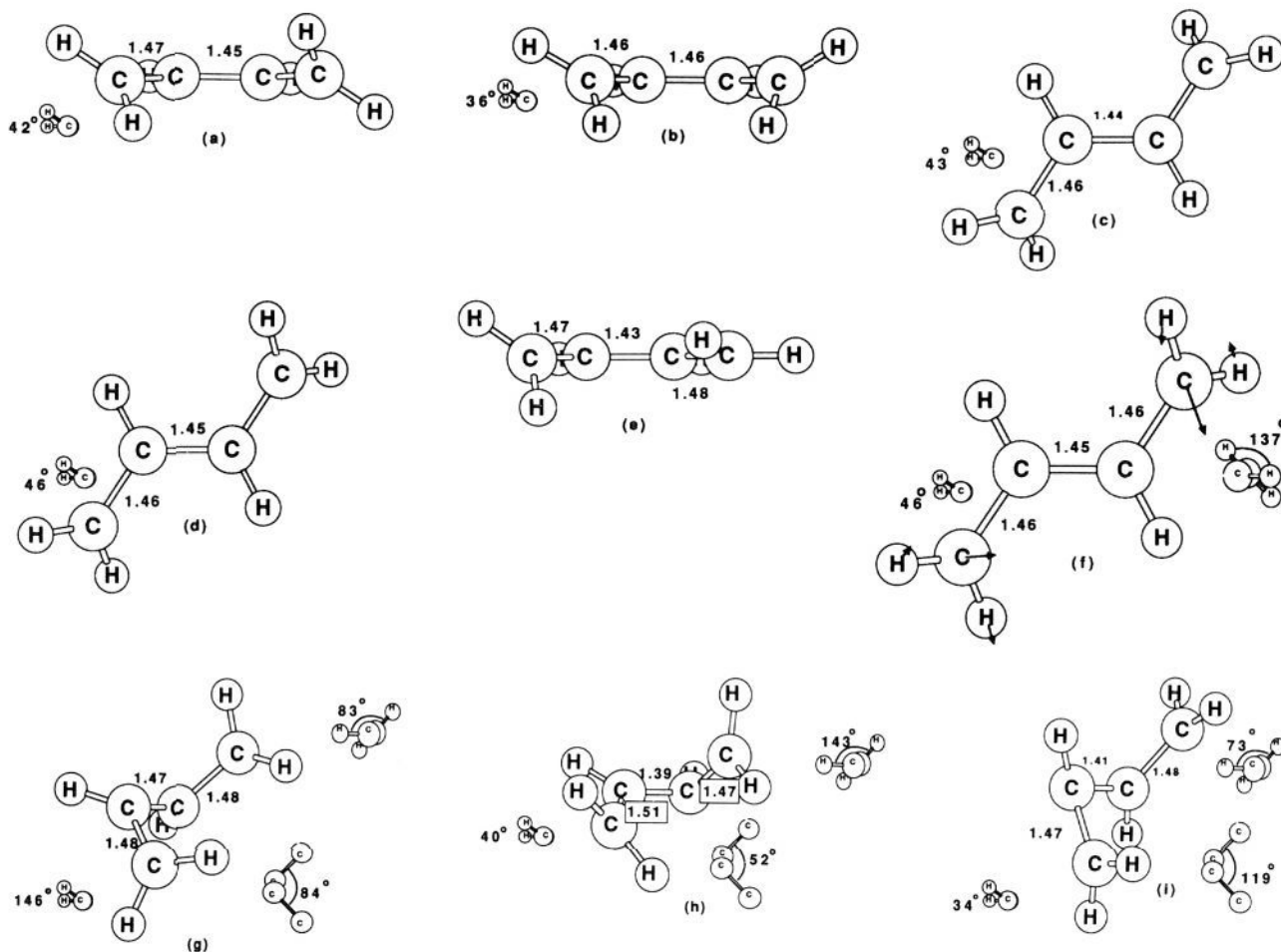


Figure 3. Optimized MC-SCF/4-31G structures: C_2 s-cis min (a), C_s s-cis min (b), C_2 s-trans min (c), S_2 s-trans min (d), C_2/C_s s-cis TS (e), C_2/S_2 s-trans TS (arrows indicate the direction of the normal mode corresponding to the imaginary frequency) (f), central CI (g), s-cisoid CI (h), and s-transoid CI (i).

each point. The energetics of these optimized structures are summarized in Table I and the geometries are collected in Figure 3g-i.

The s-transoid stationary point is connected to the s-trans basin. In fact, starting from the S_2 s-trans conformer, we immediately follow a down-hill pathway leading to this stationary point on the conical intersection (Figure 3i) which lies 3.2 kcal/mol below the S_2 s-trans minimum. This point is the lowest energy point on the excited state surface. Similarly, starting from the C_s s-cis conformer we encounter an s-cisoid stationary point on the conical intersection (Figure 3h) at 3.7 kcal/mol above the excited state minimum. In each case the pathway involves the non-synchronous rotation of the two terminal CH_2 's of butadiene in concert with the central C-C rotation. In contrast, starting from the C_2 s-trans conformer or starting from the C_2 s-cis conformer we encounter a third stationary point on the conical intersection (Figure 3g), some 6 kcal/mol above the minimum, where all the double bonds are rotated by 90° . These three conical intersection structures are stationary points on the touching region and so they give an indication of the accessibility of the conical intersection region by following the possible excited state s-cis/s-trans isomerization pathways. The location and energy of both conventional and conical intersection stationary points along these isomerization pathways is schematically illustrated in Figure 4 where the geometric parameter β (see Figure 1) is used as a pathway coordinate.

As discussed in section 2, in addition to the characterization of the conical intersection region, one needs to demonstrate that such regions are accessible via reaction paths for infinitely slow motion. These pathways have been rigorously located via ab

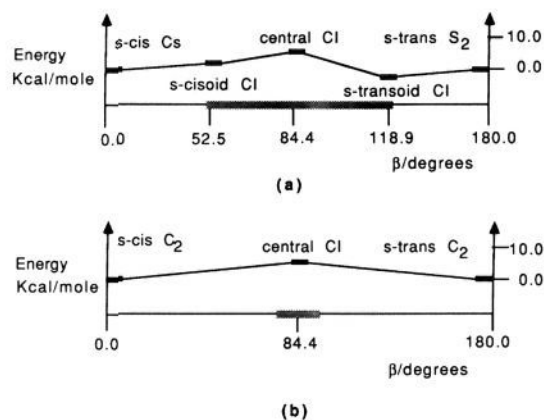


Figure 4. Schematic cross section of the energy profiles along the (a) disrotatory and (b) conrotatory s-cis/s-trans excited state isomerization pathways. The shaded region in the central part of the two profiles marks the range of the conical intersection region.

initio (MC-SCF/4-31G) calculation of the intrinsic reaction coordinate (IRC) connecting the four s-cis and s-trans minima to the conical intersection region and in turn to the conical intersection stationary points. The s-cisoid conical intersection (Figure 3h) occurs at a C-C-C-C dihedral angle of 52° while the central conical intersection (Figure 3g) is located at 84° , and the reaction paths from the C_s s-cis and S_2 s-cis minima to each conical intersection are illustrated in Figure 5a. Similarly, the s-transoid conical intersection (Figure 3i) occurs at a C-C-C-C dihedral angle of 119° , and the reaction paths from the C_2 s-trans

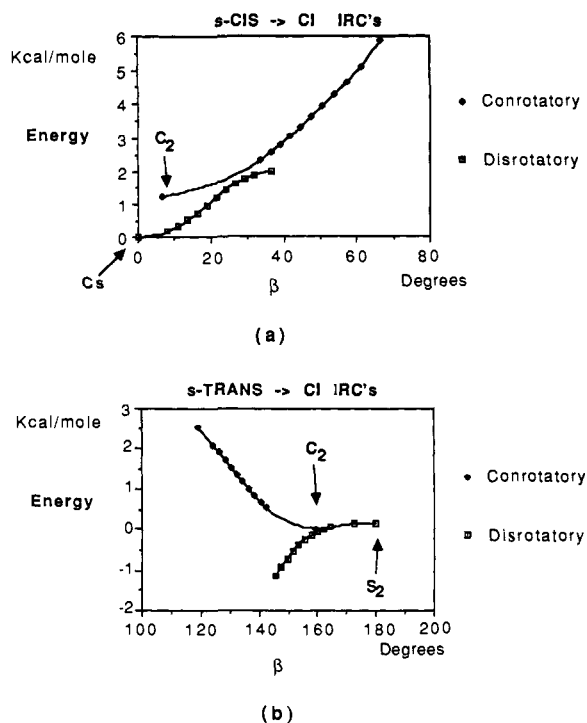


Figure 5. Energy profiles corresponding to the IRC's computed along the (a) *s-cis* \rightarrow conical intersection and (b) *s-trans* \rightarrow conical intersection excited state isomerization pathways.

and S_2 *s-trans* minima to *s-transoid* conical intersections are illustrated in Figure 5b. Figure 5 illustrates the energy profile corresponding to a pathway from each of the four excited state stationary points to the edge of the conical intersection region. The most interesting feature in Figure 5 is related to the accessibility of the conical intersection region. One can see that starting from the C_2 *s-cis* minimum or from the S_2 *s-trans* minimum the conical intersection is entered very soon along the *s-cis*/*s-trans* isomerization path near the *s-cisoid* and *s-transoid* conical intersection stationary points, respectively. These findings provide a rigorous foundation for understanding the disrotatory stereochemical preference which has been observed for butadiene photochemical ring closure which we will discuss in more detail subsequently.

A special comment needs to be made on the nature of the S_2 *s-trans* minimum. Figure 4a shows this critical point as a nonstationary point on the potential energy surface since, starting from this structure, the energy decreases along the coordinate β . In fact this coordinate dominates the lowest (59 cm^{-1}) frequency normal mode calculated for the S_2 *s-trans* optimized structure, and a very small distortion along this mode leads to a point of lower energy. Since we have not been successful in locating any transition state along this distortion, we believe that the S_2 *s-trans* stationary point can be seen as a quasi-inflection point where the system can undergo a barrierless motion toward the *s-transoid* conical intersection.

While the reaction paths and structural information just presented clearly demonstrates that the conical intersection region is accessible and thus that a model that assumes passage through a conical intersection rather than decay from an avoided crossing minimum is possible, we need to document two other aspects of the model in a quantitative fashion. Firstly, we must comment on the possibility of decay from the excited state minima, and secondly, we need to discuss the directions \mathbf{x}_1 and \mathbf{x}_2 of Scheme IV that determine the initial trajectories on the ground-state surface.

In the Oosterhoff model, one assumes that the decay originates from minima on the excited state surface. Morihashi et al.²² have studied the dynamics of this process using classical trajectories in reaction path coordinates along conrotatory and

disrotatory paths. In their approach the decay probability was computed from the non-adiabatic coupling (eq 2). The non-adiabatic coupling matrix element has two components⁴⁹ given in eq 3

$$\begin{aligned} \left\langle \Psi_1 \frac{\partial \Psi_2}{\partial s} \right\rangle &= (E_1 - E_2)^{-1} \left\langle C_1 \left(\frac{\partial H}{\partial s} \right) C_2 \right\rangle + \sum_{K,1} C_1^K C_2^K \left\langle \Phi_K \frac{\partial \Phi_L}{\partial s} \right\rangle \\ &= (E_1 - E_2)^{-1} \langle v_{12} \rangle + g_{\text{CSF}} \end{aligned} \quad (3)$$

The first component dominates and corresponds to the derivative of the CI matrix elements (which we shall refer to as the linear coupling matrix element v_{12}) divided by the energy gap $E_1 - E_2$. The second component is usually much smaller and involves the derivatives of the basis states used in the configuration interaction (CI) expansion. It is obvious that near a conical intersection point the term involving the linear coupling matrix element dominates as the energy gap approaches zero so that the non-adiabatic coupling becomes very large and the decay probability approaches one. In contrast, the decay probabilities computed by Morihashi et al.²² at the geometries of the avoided crossings are 10^{-4} and 10^{-16} for disrotatory and conrotatory ring closure, respectively. They attribute the stereospecificity to this difference (which arises mainly because of the different energy gaps for the two reaction paths). However, as we have just demonstrated, the minimum energy paths from the minima lead directly to a conical intersection where the decay probability is unity.

In addition to the photochemistry just discussed we should mention a related photophysical effect that is assumed to occur from the excited state minima: the absence of fluorescence from *s-trans*-butadiene. Zerbetto and Zgierski²¹ explain the origin of this phenomenon by computing relative decay rates of *s-trans*-butadiene through linear coupling matrix elements v_{12} multiplied by Franck-Condon factors. Since the two *s-trans* minima are separated by a 1.0 kcal/mol barrier and the S_2 *s-trans* minimum is separated from the *transoid* conical intersection by a zero barrier (the *transoid* conical intersection is the lowest energy point on the excited state surface), the whole *s-trans* region appears to be dominated by unstable structures of the system. Thus the proposed mechanism²¹ now seems unlikely since the decay to the ground state would occur via the *transoid* conical intersection within a vibrational period and no fluorescence would occur on this time scale.

We now proceed to document the nature of possible ground-state trajectories through a discussion of the vectors \mathbf{x}_1 and \mathbf{x}_2 in Scheme IV. At this stage, we view the reactivity as a quasistatic problem and are content to view the mechanism in terms of the nature of the initial trajectories in the ground state. As we have discussed in section 2, the optimized geometry of the lowest energy point on a conical intersection provides the "transition point" between the ground and excited state branch of the reaction path and is characterized by two vectors rather than one as in the case of the transition state for a thermal reaction. Thus the initial trajectories on the ground-state surface must lie in the plane defined by these two vectors \mathbf{x}_1 and \mathbf{x}_2 (computed via eqs 1 and 2) and so these vectors give an indication of the possible ground-state valleys that the system will enter and hence an indication of the possible photoproducts. We now proceed to discuss the characterization of the conical intersection region in this context.

In Figures 6–8 we give the direction of the non-adiabatic coupling matrix element (parts a and c) defined in eq 2 and the gradient difference (parts d, e, and f) for the central (Figure 6), *s-cisoid* (Figure 7), and *s-transoid* (Figure 8) conical intersections, respectively. In each figure there are three different projections: (i) parts a and d, along the central C–C bond, which give an indication of the component along the *s-cis*/*s-trans* isomerization reaction path, (ii) parts b and d, a right angle view relative to (i) (perpendicular to a plane containing the same C–C bond and the bisector of the C–C–C–C dihedral angle), which give an indication of the component along bicyclo- and cyclobutane formation

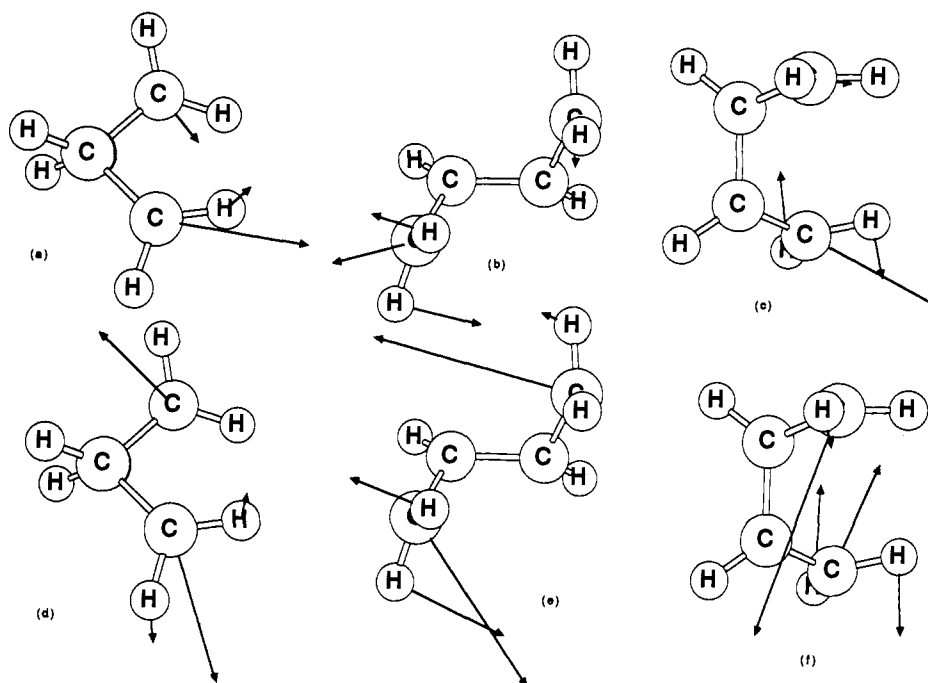


Figure 6. MC-SCF/4-31G gradient difference (a–c) and non-adiabatic coupling (d–f) for the “central” conical intersection structure.

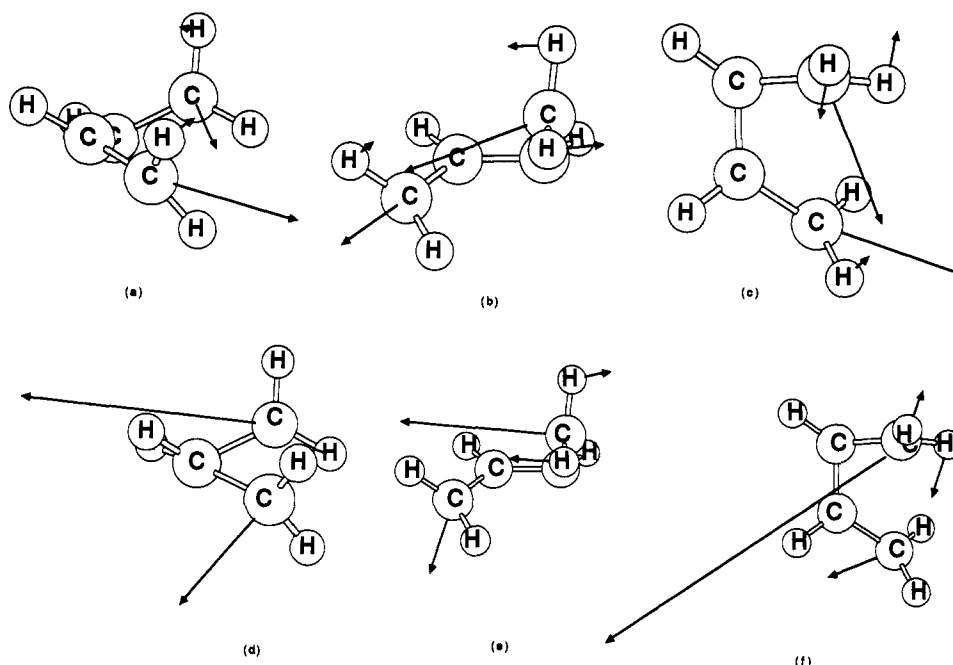


Figure 7. MC-SCF/4-31G gradient difference (a–c) and non-adiabatic coupling (d–f) for the *s*-cisoid conical intersection structure.

reaction paths, and (iii) parts c and f, a top view relative to *i* (along the perpendicular to the C–C bond that lies on the bisector of the C–C–C–C dihedral angle), which give an indication of the component along disrotatory/conrotatory CH₂ motions and the competition between three- and four-member-ring formation. For the “central conical intersection” (Figure 6) the major contributions to $\mathbf{x}_1, \mathbf{x}_2$ arise from *s*-cis/*s*-trans isomerization (Figure 6a/d), cyclo- and bicyclobutane formation (Figure 6e/f), and a CH₂ motion (Figure 6c/f) that is dominated by the motion of only one CH₂ groups but is slightly conrotatory. For the conical intersection that lies in the region of the *s*-cis minima (the *s*-cisoid conical intersection of Figure 7) one can see that the major components of $\mathbf{x}_1, \mathbf{x}_2$ lie on projections that in addition to *s*-cis/*s*-trans isomerization (Figure 7a/d) involve primarily bicyclo- and cyclobutane formation reaction paths (Figure 7c/f) with primarily disrotatory CH₂ motion (Figure 7c/f). Finally, for the lowest energy conical intersection that lies in the region of the

s-trans minima (the *s*-transoid conical intersection in Figure 8) one can see that $\mathbf{x}_1, \mathbf{x}_2$ involve primarily the *s*-cis/*s*-trans isomerization motion (Figure 7a/d) with disrotatory CH₂ motion (Figure 8b/e). Note that in the *s*-transoid conical intersection there is almost no component along the cyclobutane formation reaction paths in agreement with the experimental evidence that these paths originate from the *s*-cis conformer. We shall discuss the experimental detail in the next section. However, one can state that the dominant components of \mathbf{x}_1 and \mathbf{x}_2 are consistent with the general features of the experimental results: (a) the formation of cyclobutane occurs from the *s*-cis conformer only (compare Figure 6c/f with Figure 8c/f); (b) the major product from the *s*-trans conformer is *s*-cis/*s*-trans isomerization; (c) in general double bond isomerization is competitive with cyclobutane formation; and (d) the ring closure of butadiene is stereospecific.

To conclude this section we give a qualitative rationalization of the geometrical structures of the conical intersections and the

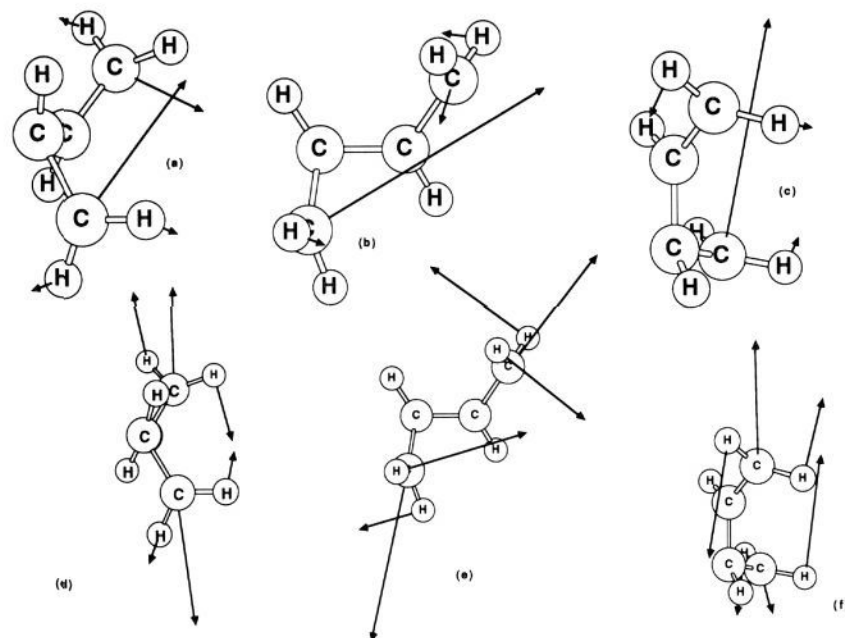


Figure 8. MC-SCF/4-31G gradient difference (a-c) and non-adiabatic coupling (d-f) for the *s*-transoid conical intersection structure.

possible ground-state pathways entered by the system which initially moves on the plane defined by x_1 and x_2 . The geometries of the three conical intersection structures (Figure 3g-i) and the corresponding MC-SCF wave functions suggest that the electronic structure at the conical intersection is, in general, that of a quasitetraradical where four unpaired electrons are almost isolated on the four carbon atoms of the butadiene framework. This tetraradical nature is obvious in the case of the central conical intersection stationary point of Figure 6 where there is an almost 90° twist about each C-C bond. However, there is still a partial tetraradical character in the *s*-cisoid and *s*-transoid conical intersections where all bonds are partially broken and where the remaining overlap between the various p^π orbitals is small. This tetraradical character is a common feature of the entire conical intersection region.

After passage through the conical intersection the system emerges at a very high energy region of the ground state potential energy surface that is located at more than 100 kcal/mol above the product region. The main reason for this difference in energy is obviously related to the lack of "bonding" in the conical intersection region due to the fact that in a tetraradical the four valence π electrons are more or less uncoupled. For infinitely slow nuclear motion, the initial ground-state trajectory in the immediate vicinity of the apex of the cone will follow some direction in the plane spanned by the vectors x_1 and x_2 which, in turn, will correlate with one of the possible spin recoupling pathways. In fact, as one moves away from the apex of the cone, the lowest energy ground state reaction valleys that may develop will be associated with energy-stabilizing processes where the four unpaired electrons will gradually recouple leading to the final formation of two new covalent bonds. In Figure 9 we give a schematic view of these spin recoupling processes for both *s*-cis- and *s*-trans-butadiene. The directions x_1 and x_2 are now easily connected to these recouplings. For example, from Figure 7 we see that in the case of the *s*-cisoid conical intersection point there are components of x_1 and x_2 for all the possible recouplings A-C in Figure 9 corresponding to cyclobutane formation coupled with asynchronous disrotatory motion of the terminal CH_2 groups and *s*-cis/*s*-trans isomerization and bicyclobutane formation.

5. Discussion

The results of the theoretical work presented in the previous sections, the global view obtained in MM-VB calculations, and

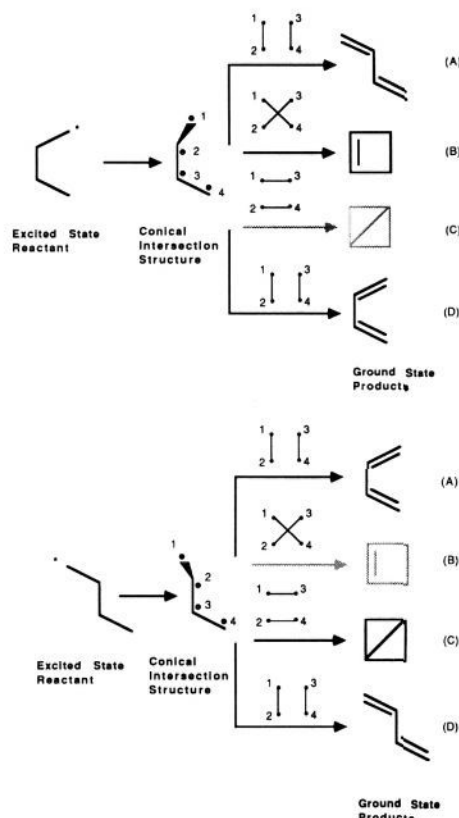
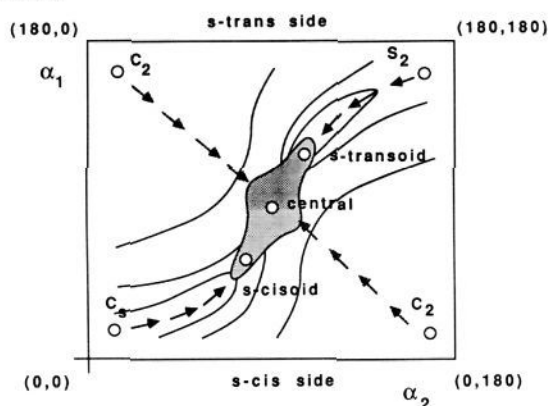


Figure 9. Possible recoupling pathways from *s*-cis and *s*-trans excited state minima.

ab initio MC-SCF/4-31G calculations all support a novel mechanistic view for the photochemical transformation of butadienes that involves passage through a conical intersection rather than decay from different avoided crossing minima. As we will now discuss, both the occurrence of several photoproducts and the stereochemical preference for the disrotatory ring closure observed in butadienes photochemistry find a natural and, in our view, unambiguous explanation on the basis of the existence and properties of the conical intersection region. The distribution of photoproducts depends on two factors: (i) the non-adiabatic transition probability which depends on the vectors x_1 and x_2 and

Scheme V

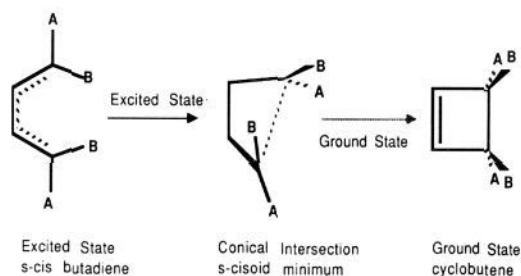


(ii) the existence of a limited number of low-energy reaction paths on the potential energy surface of the ground state that can develop as one moves away from the apex of the cone. Furthermore, the directions of the non-adiabatic coupling vector and the gradient difference vector calculated at the conical intersection stationary points and the existence of low-energy reaction paths on the excited state leading to the conical intersection give an indication of the most populated initial ground-state trajectories and hence of the accessibility of ground-state reaction valleys than can lead to a distribution of possible photoproducts.

It is convenient to structure our discussion around a schematic representation of the excited state potential surface and conical intersection region defined in the cutting plane of Figure 1. This can be constructed on the basis of the global views presented in Figure 2 and the reaction paths presented in Figure 5 and is illustrated in Scheme V.

We begin with a discussion of the decay from the *s-cis* region (see also Figure 1 for reference). On the excited state branch of the reaction path, the system, after photoexcitation, undergoes a relaxation process leading to the low-energy region of the potential energy surface where the excited state minima and the conical intersection region are located and a very rapid passage to the ground state potential energy surface is possible. There are two stereochemically different pathways connecting the two *s-cis* minima (C_1 and C_2) to the conical intersection region. Along the disrotatory pathway (the one starting from the C_1 minimum) the system enters the conical intersection region, located 4 kcal/mol above the minimum, with a value of β below 50° (see Figures 4 and 5). The situation is different along the conrotatory pathway, where the system enters the central conical intersection region, about 6 kcal/mol above the minimum, with a value of the β torsional angle larger than 80° . As shown in Scheme V the location of the edge of the conical intersection (dotted area) is consistent with an immediate passage into the conical intersection region and thus to the ground state when the system moves along the disrotatory pathway while the conrotatory pathway corresponds to a less favorable route. From a more chemical point of view this means that we should expect a high degree of stereospecificity during the ring closure of substituted butadienes. As illustrated in Scheme VI an excited state *s-cis*-butadiene enters the conical intersection region in a conformation already consistent with the production of only one ground-state cyclobutene isomer. One can conclude that the stereochemical decision is taken mainly on the excited state branch of the reaction pathway since the low-energy pathway corresponds to disrotatory motion. The ground-state branch of the reaction path involves mainly the formation of the two new covalent bonds since x_1 and x_2 from Figure 7 are dominated by ring closure and rotation about the central C–C bond coupled with disrotatory motion of the two terminal CH_2 . Remarkably the direction of x_1 and x_2 is very different in case of a passage through the “central” stationary point where only one of the two methylene groups is rotating (see Figure 6).

Scheme VI



In the case of *s-trans*-butadiene, the excited state branch of the reaction path corresponds to the same *s-cis*/*s-trans* isomerization motion but, of course, in the opposite direction with respect to the one followed by the *s-cis* form (see Figure 8). Again, the *s-trans*-butadiene will first enter the conical intersection region along the disrotatory pathway at a point (the *s-transoid* stationary point) located well before the “central point” of the conical intersection and corresponding to the absolute minimum of the 2^1Ag excited state potential energy surface. In this case the nature of x_1 and x_2 is different from that of the *s-cis* reaction, with the important motion being the component of *s-cis*/*s-trans* isomerization. In fact, Squillacote et al. have demonstrated experimentally⁴ that cyclization occurs, simultaneously to double-bond isomerization, when *s-cis*-2,3-dimethylbutadiene (*s-cis*-DMB) is irradiated at temperatures between 10 and 20 K while no such reaction is observed in *s-trans*-DMB. Furthermore, this result shows that DMB and the parent butadiene photoreact even when the system is vibrationally cold on the electronically excited state and that, as a consequence, this reaction should be almost barrierless. The same low-temperature reactivity has been found in the *s-cis*/*s-trans* isomerization reaction.^{5,6}

The “recoupling” process discussed in the previous section and illustrated schematically in Figure 9 will dominate the ground-state stage of the reaction which starts at the conical intersection region and ends in one of the ground-state minima corresponding to a photoproduct. The different recoupling pathways will be differentially populated according to the particular geometric structure of the conical intersection point where the decay occurs (i.e. *s-cisoid*, central, etc.) and the detailed nature and population of the initial ground-state trajectories which lies on the specific plane x_1x_2 centered on the conical intersection point itself. For example, as we have already discussed in section 2, the excited state branch of the reaction pathway enters the conical intersection in the direction of x_1 corresponding to the gradient difference (eq 1) which normally points to the apex of the cone. While, adiabatically, the system will tend to follow this same direction of motion in the ground-state sheet, a specific ground-state initial trajectory will deflect (i.e. “rotate” on the plane x_1x_2) depending on the direction and magnitude of the non-adiabatic coupling vector x_2 .^{36–38} This leads to the prediction that a certain fraction of the ground-state reaction pathways actually followed by the system will not run along the same direction of the excited state pathway branch from which it originates but will continue in directions leading to different photoproducts. In particular, one is led to predict that substituents and environment of the butadiene moiety will control the way in which the system enters and exits the conical intersection region. The observed quantum yields for the different simultaneous butadiene photoproducts seem to be in line with this prediction as we will now discuss.

As we have previously demonstrated, the excited state branches of the reaction path for *s-cis*- and *s-trans*-butadiene enter the conical intersection region along a reaction path that involves mainly the rotation about the central C–C bond coupled with asynchronous disrotatory motion of the terminal methylenes. If this excited state reaction path simply continued on the ground state then the major products would be the result of *s-cis*/*s-trans* isomerization and double bond *cis*/*trans* isomerization. Indeed these are the major products of the photochemistry. However,

s-cis- and *s-trans*-butadiene enter the conical intersection region at different geometries where the nature of x_1 and x_2 are different. As a consequence, the distribution of minor photoproducts from *s-cis*- and *s-trans*-butadiene will be rather different. For example, since *s-cis*-butadiene enters the conical intersection at less than 90° in the central C–C torsional angle, the formation of the four-member-ring product (cyclobutene) will be highly probable while the formation of the more strained three-member-ring product is unfavored, and this idea has its quantitative expression in the directions of x_1 and x_2 . The facile *s-cis*/*s-trans* isomerization leading to *s-trans*-butadiene and double bond *cis*/*trans* isomerization plus *s-cis*-butadiene back-formation leading back to *s-cis*-butadiene, on the other hand, are rationalized by a reaction path on the ground state that is the continuation of the initial excited state path. In contrast, *s-trans*-butadiene enters the conical intersection when the value of the β angle is larger than 90° thus making the formation of cyclobutene highly improbable so that the only possible *s-trans*-butadiene cyclic photoproduct will be bicyclobutane. The directions of x_1 and x_2 again give the quantitative expression of these ideas. For *s-trans*-butadiene, facile *s-cis*/*s-trans* isomerization and the process leading to *s-trans*-butadiene back-formation would again correspond to the continuation of the original excited state reaction path.

Thus our results demonstrate that the origin and simultaneous formation of all the experimentally observed photoproducts of butadiene can be readily rationalized on the basis of the reaction network discussed above and the recoupling paths in Figure 9. In other words, the different fractions of the initial photoexcited reactant, either *s-cis*- or *s-trans*-butadiene, will follow different pathways, each one associated with a distinct electron recoupling process. In this way it is easy to rationalize the simultaneous production of different photoproducts and the sensitivity of quantum yields measurements to the type of substitution or the type of environment in which the butadiene moiety is embedded.

The pool of experimental data indicates that the photochemistry of butadienes is rather complex. Direct irradiation of butadienes in dilute solution with a 254-nm light source leads to *s-cis*/*s-trans* isomerization, double bond *cis*–*trans* isomerization, cyclobutenes, bicyclo[1.1.0]butane, and 1-methylcyclopropene formation.^{1–15} While the specific quantum yields of the corresponding products depend on the particular structure of the reacting butadiene (i.e. cyclic or acyclic butadienes, and type, position, and number of substituents in the butadiene moiety), the products seem to be formed simultaneously during the reaction. For example, *s-cis*/*s-trans* isomerization in butadiene, isoprene, and 2-isopropyl butadiene has been proved to be a process faster than cyclobutane formation.^{4–6} On the other hand, the efficiency of *s-cis*/*s-trans* isomerization decreases dramatically in 2,3-disubstituted butadienes such as 2,3-dimethylbutadiene (DMB) where both cyclobutane formation and double bond *cis*/*trans* isomerization occur about fifty times faster.⁴ Bicyclo[1.1.0]butane is formed in low quantum yield during butadiene cyclization along with other substituted acyclic and cyclic butadienes^{7–10} while 1,3-dimethylcyclopropene is formed, via the same hypothetical biradical intermediate leading to bicyclo[1.1.0]butane (see eq 4 in Scheme I), during direct irradiation of *cis*- and *trans*-1,3-pentadiene.¹⁵

The general capacity of an acyclic *s-cis*-butadiene to photoreact seems to be related to the resistance of the central C–C bond of the butadiene moiety to undergo rotation.^{12,13} Rigid butadienes

such as 2,3-dimethylenebicyclo[2.2.1]heptane or 1,2-dimethylenecyclobutane have low quantum yield for the disappearance of the diene (0.025 and <0.01 , respectively) in comparison to less rigid molecules such as 1,2-dimethylenecyclopentane and 1,2-dimethylenecyclohexane (quantum yields 0.11) or almost freely rotating butadienes such as 2,3-dimethylbutadiene. This behavior has a natural explanation if we consider that the excited state butadiene moiety needs to rotate about the central C–C bond in order to reach at least the edge of the conical intersection region where it can decay to the ground state. From our results, one can predict that in order to photoreact, the butadiene moiety must probably undergo a rotation larger than 40° about the central C–C bond simultaneously to terminal methylene rotations.

With the same kind of argument one can also explain the observed quantum yield trends for the photoproduction of bicyclo[1.1.0]butane. This compound, which is usually a side product (quantum yield ratio 16:1 in iso-octane) of the photocyclization of butadiene to cyclobutene,^{7–10} becomes the major photoproduct in systems where the butadiene moiety is constrained near an *s-trans* conformation or when certain catalysts are used.^{3,11} In this case the butadiene moiety will, during the first stage of the reaction, distort toward the quasitetraradical structure from the *s-trans* minima region. The passage to the ground state will then follow the pathway associated with the most favorable spin recoupling process. A framework which favors the *s-trans* conformation in the butadiene moiety will obviously disfavor the recoupling of the two terminal methylene unpaired electrons (requiring an almost 180° rotation about the C–C central bond) leading to cyclobutene. In contrast, the recoupling of the electron pairs 1,3 and 2,4 requires only a central C–C rotation up to the conical intersection region together with terminal methylene rotation.

6. Conclusions

In this work we have presented a detailed study of the 2^1A_g potential energy surface of butadiene. While the minima on the excited state surface have been studied in other work, here we have shown that the computed reaction paths from the excited state minima lead to conical intersections where the system can decay within a single vibrational period. The lowest energy path from the *s-trans* minimum on the 2^1A_g potential energy surface involves the rotation of the central C–C bond coupled with asynchronous disrotatory motion of the terminal methylenes and leads to an *s-transoid* conical intersection region without passing over a barrier. The path from *s-cis* leads to an *s-cisoid* conical intersection that lies some 4 kcal mol^{-1} above the minima. The nature of the possible reaction paths on the excited state is consistent with the fact that the major products of the photochemical reactions of butadiene are the facile *s-cis*/*s-trans* isomerization and double bond *cis*/*trans* isomerization. The conical intersection points have been characterized by computing the gradient difference and non-adiabatic coupling vectors. The directions of the gradient difference and non-adiabatic coupling vectors are consistent with the production of cyclobutenes as minor products.

Acknowledgment. This research has been supported by the SERC (UK) under Grant No. GR/G 03335. The authors are also grateful to IBM for support under a Joint Study Agreement. All computations were run on an IBM RS6000.